

MISSING NUCLEON RESONANCES IN KAON PRODUCTION WITH PIONS AND PHOTONS

C. BENNHOLD, A. WALUYO, H. HABERZETTL

*Center for Nuclear Studies, Department of Physics, The George Washington
University,
Washington, D.C. 20052, USA
E-mail:bennhold@gwu.edu*

T. MART

*Jurusan Fisika, FMIPA, Universitas Indonesia,
Depok 16424, Indonesia*

G. PENNER, U. MOSEL

*Institut für Theoretische Physik, Universität Giessen,
D-35392 Giessen, Germany*

Resonances with strong couplings to strangeness channels are investigated in a coupled-channels framework of kaon production with pions and photons. We find evidence for an additional D_{13} resonance around 1900 MeV that has a significant decay width into the $K\Lambda$ final state. Such a state has been predicted in a relativistic quark model at 1960 MeV with significant γN and $K\Lambda$ branching ratios.

1 Introduction

Like any composite system the nucleon can be excited into a number of resonant or compound states. However, due to the nonperturbative nature of QCD at nucleon resonance energies no rigorous understanding of N^* resonances on the basis of QCD has emerged. Lattice QCD has only recently begun to contribute to this field. In a recent study ¹ the excitation energies of $1/2^-$ and $3/2^-$ baryon resonances are calculated for the first time on the lattice with improved actions. On the other hand, quark models that contain three constituent valence quarks predict a much richer resonance spectrum ^{2,3} than has been observed in $\pi N \rightarrow \pi N$ scattering experiments. Quark model studies have suggested that those "missing" resonances may couple strongly to other channels, such as the $K\Lambda$ and $K\Sigma$ channels ⁴ or final states involving vector mesons. While most of the present information on nucleon resonances has been obtained in $\pi N \rightarrow \pi N$ experiments the advent of the newly established electron and photon facilities have made it possible to investigate the mechanism of nucleon resonance excitation with photons and electrons. Experiments producing kaon-hyperon final states have been performed at ELSA ⁵ and are being analyzed at JLab.

2 Kaon Photoproduction at Tree Level

Within the one-photon approximation, the full amplitude for any photoproduction process can be written in terms of a Bethe-Salpeter equation

$$M = V + V G T, \quad (1)$$

where V represents the driving term for the particular photoproduction process, G is the meson-baryon two-particle propagator, and T is the hadronic meson-baryon final state interaction. In principle, one would have to solve this equation as a four-dimensional integral equation. However, most studies over the last 30 years have analyzed the $N(\gamma, K)\Lambda(\Sigma)$ reactions in a tree-level isobar framework⁶, neglecting the hadronic final state interaction in Eq. 1. Without rescattering contributions the T -matrix is simply approximated by the driving term alone which is assumed to be given by a series of tree-level diagrams whose couplings were adjusted to reproduce the experimental data. Due to the poor data quality it was not possible to decide which resonances contributed, even the background terms could not be modelled properly, i.e., if standard SU(3) coupling constants were used for the leading $g_{K\Lambda N}$ and $g_{K\Sigma N}$ couplings the calculations overpredicted the data by an order of magnitude. The recent work on including hadronic form factors in photoproduction reactions⁷ while maintaining gauge invariance has resulted in the proper description of the background terms, allowing the use of approximate SU(3) symmetry to fix the Born coupling constants $g_{K\Lambda N}$ and $g_{K\Sigma N}$.

Here, we use as a starting point the tree-level isobar model described in Ref.^{8,9} to analyze the $p(\gamma, K^+)\Lambda$ process in more detail. Guided by a recent coupled-channels analysis¹⁰, the low-energy resonance part of this model includes three states that have been found to have significant decay widths into the $K^+\Lambda$ channel, the $S_{11}(1650)$, $P_{11}(1710)$, and $P_{13}(1720)$ resonances. The background part includes the standard Born terms along with the $K^*(892)$ and $K_1(1270)$ vector meson poles in the t -channel. As in Ref.⁸, we employ the gauge method of Haberzettl⁷ to include hadronic form factors.

The new SAPHIR total cross section data⁵ for the $p(\gamma, K^+)\Lambda$ channel, shown in Fig. 1, indicate for the first time a structure around $W = 1900$ MeV. This structure could not be resolved before due to the low quality of the old data. While there are no 3- or 4-star isospin 1/2 resonances around 1900 MeV in the Particle Data Book¹¹, several 2-star states are listed. Of those only the $D_{13}(2080)$ has been identified in older $p(\pi^-, K^0)\Lambda$ analyses^{12,13} to have a noticeable branching ratio into the $K\Lambda$ channel. On the theoretical side, the constituent quark model by Capstick and Roberts³ predicts many new states around 1900 MeV, however, only a few of them have been calculated to

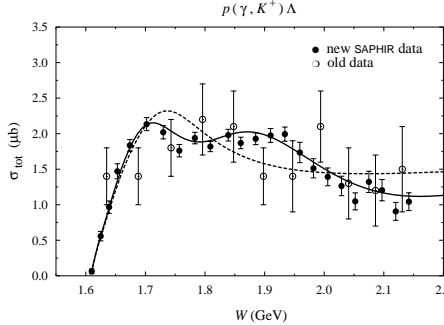


Figure 1: Total cross section calculations for $K^+\Lambda$ photoproduction on the proton obtained at tree level. The dashed line shows the result without the new $D_{13}(1900)$ resonance, while the solid line is obtained by including the new $D_{13}(1900)$ state. The new SAPHIR data⁵ are denoted by the solid circles.

have a significant $K\Lambda$ decay width⁴. These are the $[S_{11}]_3(1945)$, $[P_{11}]_5(1975)$, $[P_{13}]_4(1950)$, and $[D_{13}]_3(1960)$ states, where the subscript refers to the band that the state is predicted in. As discussed in more detail in ref. ⁹ we have performed fits for each of these possible states, allowing the fit to determine the mass, width and coupling constants of the resonance. While all four of the above resonances have large decay widths into the $K\Lambda$ channel, only the $D_{13}(1960)$ state is predicted to also have significant photocouplings. Table 1 presents the remarkable agreement, up to the sign, between the quark model prediction and our extracted results for the $D_{13}(1960)$. For the other three states the partial widths extracted from our fit overestimate the quark model results by up to a factor of 30. Figure 1 compares our models with and without the $D_{13}(1960)$ with the SAPHIR total cross section data⁵. Our result without this resonance shows only one peak near threshold, while inclusion of the new resonance leads to a second peak at W slightly below 1900 MeV, in agreement with the new SAPHIR data⁵. As shown in Ref.⁹, the difference between the two calculations is smaller for the differential cross section and the recoil polarization.

3 Kaon Production in a Coupled Channels K-matrix Approach

Going beyond tree level requires inclusion of the rescattering term in Eq. 1. To simplify the integral equation one can rewrite the full Bethe-Salpeter equation in the form

$$K = V + V \operatorname{Re}(G_{\text{BS}})K \quad (2)$$

Table 1: Comparison between the results from our tree-level fit to the $p(\gamma, K^+) \Lambda$ data and those of the quark model (QM), where the QM photocouplings were taken from Ref.¹⁴ and the $K\Lambda$ decay widths from Ref.⁴.

Missing Resonance	Model	m_{N^*} (MeV)	Γ_{N^*} (MeV)	$\sqrt{\Gamma_{N^* N\gamma} \Gamma_{N^* K\Lambda}} / \Gamma_{N^*}$ (10^{-3})
D_{13}	Fit	1895	372	$2.292^{+0.722}_{-0.204}$
	QM	1960	535	-2.722 ± 0.729

$$T = K + iK \operatorname{Im}(G_{BS})T . \quad (3)$$

where G_{BS} is the full propagator. Any truncation of the first equation will still provide a unitary, albeit approximate, solution, as long as $i \operatorname{Im}(G_{BS})$ correctly describes the discontinuity across the scattering cut. Taking the special choice of placing both intermediate particle on shell leads to $K = V$ and simple K-matrix (Born) approximation:

$$T = \frac{V}{1 - iV} . \quad (4)$$

This procedure still allows for the resonance widths to be generated dynamically, while the real part of the self-energy is absorbed in an effective resonance mass that is determined by the fit. Enforcing unitarity dynamically therefore requires solving a system of coupled channels with all possible final states. The most recent work that employs the K -matrix approximation within an effective Lagrangian framework has been performed by Feuster and Mosel¹⁰. They extract nucleon resonance parameters by simultaneously analyzing all available data for reactions involving the initial and final states $\gamma N, \pi N, \pi\pi N, \eta N$ and $K\Lambda$ up to $W = 1.9$ GeV.

Here we extend the approach of Ref.¹⁰ to study resonances around 1900 MeV in more detail. We have extended the energy range up to 2.0 GeV and included the $K\Sigma$ final state. Our best fit to all hadronic data of the reactions $\pi N \rightarrow \pi N, \pi N \rightarrow \pi\pi N, \pi N \rightarrow \eta N, \pi N \rightarrow K\Lambda$ and $\pi N \rightarrow K\Sigma$ indeed does result in three D_{13} excitations, the well-known $D_{13}(1520)$ state, the 3-star $D_{13}(1700)$ state and a new D_{13} state at 1945 MeV with a large width of 583 MeV. Figure 2 shows our description of the $D_{13} \pi N$ partial wave; the prominent $D_{13}(1520)$ is clearly visible, the $D_{13}(1700)$ is not apparent, while the inclusion of another state around 1900 MeV clearly improves the agreement in

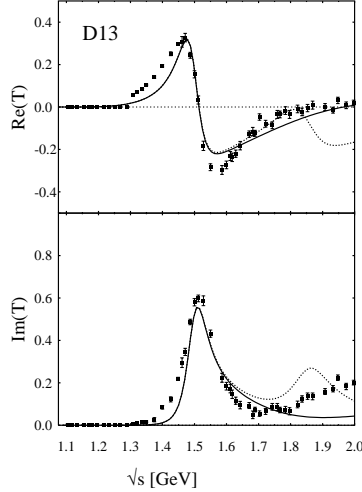


Figure 2: The D_{13} phase calculated in the coupled-channels K-matrix approach, fitted to the SM95 PWA. The solid line includes the new $D_{13}(1900)$ state while the dashed line does not.

the real part which exhibits a zero crossing at that energy. The imaginary part, on the other hand, is missing some strength, possibly indicating the threshold opening of a channel that is not included.

Fig. 3 displays differential cross sections for the $\pi^- p \rightarrow K^0 \Lambda$ reaction at different W . While the signal is small there is a clear improvement in the description of the data when the new D_{13} state is included. Unfortunately, the total cross section data for the same reaction, shown in Fig. 4, are much too poor to distinguish between the two cases.

Is this state identical to the 2-star resonance $D_{13}(2080)$ listed in the Particle Data Table? Table 2 displays a list of D_{13} states below 2.1 GeV predicted by Refs.^{3,4}, along with the Particle Data Table listings and the states found in our fit within the K-matrix approach. A closer examination of the literature reveals that there has been some evidence for two resonances in this partial wave between 1800 and 2200 MeV¹⁵; one with a mass centered around 1900 MeV and another with mass around 2080 MeV. It is the former which has been seen prominently in two separate $p(\pi^-, K^0)\Lambda$ analyses^{12,13}. Thus, even though the remarkable quantitative agreement is probably fortuitous, we believe that the structure seen in the SAPHIR data is in all likelihood identical to the one seen in hadronic $K\Lambda$ production and, furthermore, corresponds to the $D_{13}(1960)$ state predicted by the quark model. The D_{13} excitation around 2080 MeV

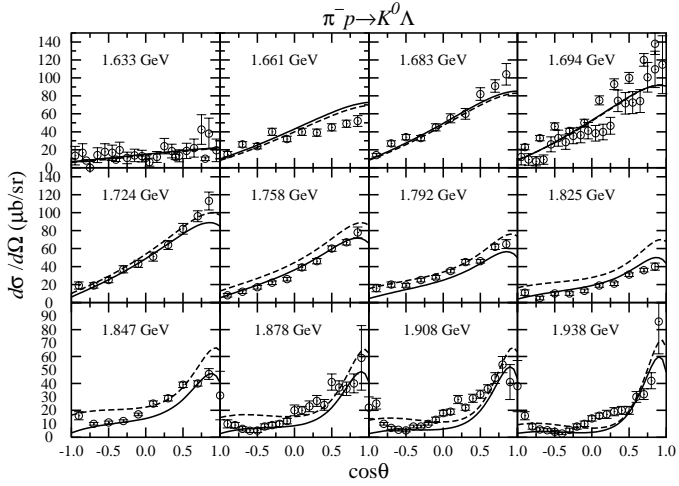


Figure 3: Differential cross section calculations for the $p(\pi^-, K^0)\Lambda$ reaction in the coupled-channels approach. The notation of the curves is as in Fig. 2.

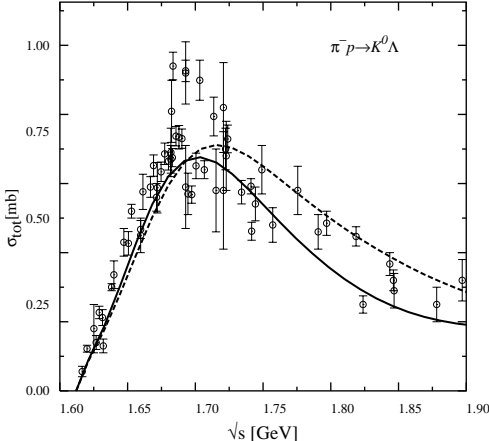


Figure 4: Total cross section calculations for the $p(\pi^-, K^0)\Lambda$ reaction in the coupled-channels approach. The notation of the curves is as in Fig. 2.

seen in Ref.¹⁵ may well correspond to the quark model state $D_{13}(2055)$ in the $N = 4$ band.

In order to clearly separate these nearby D_{13} states, measuring other channels will be helpful. For example, Ref.³ predicts the $D_{13}(1960)$ to have large

Table 2: Summary of listed D_{13} resonances. The observed states from the Particle Data Table are ordered according to Refs.^{3,4} and compared to our fit.

Quark Model ^{3,4}	Particle Data Table ¹¹	our fit
$[N\frac{3}{2}^-]_1(1495)$	$D_{13}(1520)(****)$	$D_{13}(1520)$
$[N\frac{3}{2}^-]_2(1625)$	$D_{13}(1700)(***)$	$D_{13}(1706)$
$[N\frac{3}{2}^-]_3(1960)$	$D_{13}(2080)(**)$	$D_{13}(1945)$
$[N\frac{3}{2}^-]_4(2055)$	-	-
$[N\frac{3}{2}^-]_5(2095)$	-	-

decay widths into the ηN and $\eta' N$ channels, in contrast to the $D_{13}(2055)$ whose branching ratios into these channels are negligible.

What other experiments can help uncover the role played by this resonance? The largest effects are found in the photon asymmetry shown in Fig. 5. For $W \geq 1800$ MeV, including the new resonance leads to a sign change in the photon asymmetry whose magnitude is almost 100 percent at intermediate angles. Clearly, measuring this observable is well suited to shed more light on the contribution of this state in kaon photoproduction. Ultimately, only a detailed multipole analysis can verify that the observed structure is indeed due to a resonance. With the arrival of new, high-precision cross section and polarization data the kaon photoproduction process will be able to unfold its full potential in the search and study of nucleon resonances.

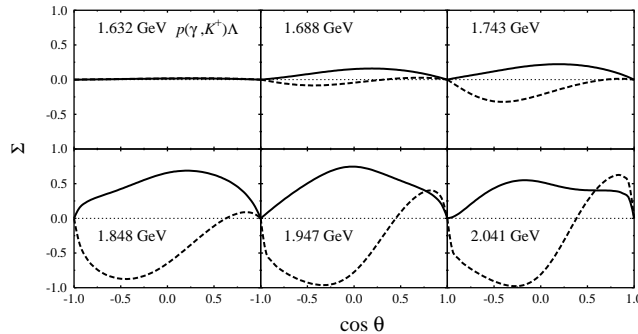


Figure 5: Polarized photon asymmetry for the $p(\gamma, K^+)\Lambda$ reaction. The notation of the curves is as in Fig. 2.

Acknowledgments

This work was supported by US DOE grant DE-FG02-95ER-40907 (CB, AW, and HH), the University Research for Graduate Education (URGE) grant (TM), and the DFG and GSI Darmstadt in Germany (GP and UM).

References

1. F. X. Lee and D. B. Leinweber, Nucl. Phys. Proc. Suppl. **73**, 258 (1999) (hep-lat/9809095 (1998)).
2. N. Isgur and G. Karl, Phys. Lett. B **72**, 109 (1977); Phys. Rev. D **23**, 817 (1981); R. Koniuk and N. Isgur, Phys. Rev. D **21**, 1868 (1980).
3. S. Capstick and W. Roberts, Phys. Rev. D **49**, 4570 (1994).
4. S. Capstick and W. Roberts, Phys. Rev. D **58**, 074011 (1998).
5. SAPHIR Collaboration: M. Q. Tran *et al.*, Phys. Lett. B **445**, 20 (1998).
6. R. A. Adelseck, C. Bennhold, and L. E. Wright, Phys. Rev. C **32**, 1681 (1985); R. A. Williams, C.-R. Ji, and S. R. Cotanch, Phys. Rev. C **46**, 1617 (1992); J. C. David, *et al.* Phys. Rev. C **53**, 2613 (1996).
7. H. Haberzettl, C. Bennhold, T. Mart, and T. Feuster, Phys. Rev. C **58**, R40 (1998); H. Haberzettl, Phys. Rev. C **56**, 2041 (1997).
8. C. Bennhold *et al.*, in *Proceedings of the Workshop on Electron Nucleus Scattering*, Elba, Italy, 1998, (edited by O. Benhar, A. Fabrocini, and R. Schiavilla, Edizioni ETS, Pisa, 1999) p. 149; F.X. Lee *et al.*, nucl-th/9907119.
9. T. Mart and C. Bennhold, Phys. Rev. C **61**, 012201(R) (1999).
10. T. Feuster and U. Mosel, Phys. Rev. C **58**, 457 (1998); **59**, 460 (1999).
11. C. Caso *et al.*, Eur. Phys. J. C **3**, 1 (1998).
12. D. H. Saxon *et al.*, Nucl. Phys. **B162**, 522 (1980).
13. K. W. Bell *et al.*, Nucl. Phys. **B222**, 389 (1983).
14. S. Capstick, Phys. Rev. D **46**, 2864 (1992).
15. R. E. Cutkosky, *et al.*, Phys. Rev. D **20**, 2839 (1979); G. Höhler, F. Kaiser, R. Koch, E. Pietarinen, Physics Data, No. 12-1 (1979).